Majorana Feynman rules

Evalyn I. Gates
Department of Physics, Case Western Reserve University, Cleveland, Ohio 44106

Kenneth L. Kowalski*
High Energy Physics Division, Argonne National Laboratory, Argonne, Illinois 60439
(Received 22 May 1987)

Nontrivial relative-sign ambiguities are pointed out in previous statements of the Feynman rules for field theories containing Majorana fermions. New graphical rules which resemble those for Dirac fermions in their natural association of momentum and fermion flows are proposed that have only those signature problems normally expected for fermions. The new rules utilize only the conventional fermion propagator and involve vertices without appended charge-conjugation matrices. The number of two-Majorana–boson vertices is reduced from six to two.

I. INTRODUCTION

Majorana fermions have long been of interest as possible facilitators of neutrinoless double-beta decay. More recently it has been found that Majorana fermions appear in a number of proposed extensions of the standard model. In view of this interest in the possibility of their observation and special attributes,[1] it is surprising that there have been relatively few detailed discussions[2–4] of the unusual aspects of Majorana Feynman rules that result from Majorana fermion self-conjugacy.

The usual statements[3,4] of Majorana Feynman rules differ from those for Dirac fermions in the appearance of three different propagators and a related multiplicity of vertices. The self-conjugacy of Majorana fermions is responsible not only for these differences, but also for ambiguities in the spinor assignments for external lines, in the appropriate choices of propagators and directions of momentum flows for internal lines, and finally, in the relative signatures of the various graphs contributing to a given amplitude.

All of these difficulties are addressed in Refs. 3 and 4. Nonetheless, for amplitudes of sufficient complexity the question of the relative signs of different graphs contributing to the same amplitude is not settled.[5] For example, in the photino bremsstrahlung calculations carried out in Ref. 5 direct recourse to Wick's theorem was necessary in order to resolve signature ambiguities. This tactic, while unequivocal, plainly defeats the original purpose in stating graphical rules. With this in mind we develop a new set of Feynman rules for field theories containing Majorana fermions that involves the standard fermion propagator, fewer and simpler vertices, and only the familiar signature-assignment problems that are encountered in theories containing only Dirac fermions. This provides an interesting as well as a seemingly less ambiguous alternative to previous treatments of Majorana fermions in perturbation theory.

For the sake of simplicity, as well as to allow us to appropriate several examples already worked out in Ref. 5, we use the model of Wess and Zumino[6] for supersymmetric quantum electrodynamics (SUSY QED) in the main body of the text. Most of the issues with which we are concerned can be clearly addressed in the language of this model. The generalization to more general Majorana couplings, including the boson–double-Majorana couplings that are not present in the Wess-Zumino model, is outlined in the Appendix.

II. WESS-ZUMINO MODEL

If the auxiliary gauge field is eliminated, the Lagrangian for the Wess-Zumino[6] model is

$$\mathcal{L}_{\mathrm{WZ}}=\mathcal{L}_G+\mathcal{L}_Q+\mathcal{L}_{\mathrm{SY}} . \tag{2.1}$$

Only the photons A_μ and the photino λ, which is a Majorana fermion, appear in the noninteracting gauge-field part of $\mathcal{L}$:

$$\mathcal{L}_G=-\tfrac{1}{4}F_{\mu\nu}F^{\mu\nu}+\tfrac{1}{2}i\bar{\lambda}\partial\!\!\!/\lambda . \tag{2.2}$$

The charged-particle QED Lagrangian $\mathcal{L}_Q$ contains a scalar (S), pseudoscalar (P), and Dirac fermion (ψ) contributions

$$\mathcal{L}_Q=(D_\mu S^\dagger)(D^\mu S)+m^2S^\dagger S+(D_\mu P^\dagger)(D^\mu P) +m^2P^\dagger P+\bar{\psi}(iD\!\!\!/-m)\psi , \tag{2.3}$$

where $D_\mu=\partial_\mu+iQA_\mu$ and $F_{\mu\nu}=\partial_\mu A_\nu-\partial_\nu A_\mu$. The remainder of $\mathcal{L}$ contains the interaction terms that arise on account of the gauge supersymmetry,

$$\mathcal{L}_{\mathrm{SY}}=iQ[\bar{\psi}(S+i\gamma_5P)\lambda-\bar{\lambda}(S^\dagger+i\gamma_5P^\dagger)\psi] +\tfrac{1}{2}Q^2(S^\dagger P-SP^\dagger)^2 , \tag{2.4}$$

namely, the coupling of the photino to the charged fields as well as the quartic interaction resulting from the elimination of the auxiliary gauge field. Whether the photino is massless or not is irrelevant to our considerations, although it must be massless for the realization of supersymmetry. Both the ψ and λ fields transform as four-component spinors under the Lorentz group.

We follow the conventions of Ref. 7 for the metric and Majorana representation ($\gamma^{\mu *}=-\gamma^{\mu}$) of the γ matrices except for our choice of phase for the charge-conjugation matrix which we take as

$$C=-\gamma^0 . \tag{2.5}$$

In the Majorana representation

$$C=-C^T=C^{\dagger}=C^{-1}=-C^* , \tag{2.6}$$

where T, $\dagger$, and $*$ denote the transpose, Hermitian adjoint, and complex-conjugation operation, respectively, on the spinor space. With these conventions the positive- and negative-energy, four-component, plane-wave spinors are related by

$$v(p,\eta)^*=u(p,-\eta) , \tag{2.7}$$

where $\eta=\pm 1$ is a polarization index.[3] Equation (2.7) is solely a consequence of the choice of the Majorana representation for the γ matrices and does not imply that u and v are spinors that refer only to Majorana fermions. The same spinors are employed in the plane-wave representations of both the ψ and λ fields.

The self-conjugate property of the photino field implies that its spinor components are Hermitian with respect to the adjoint operation on the full Hilbert space, namely,

$$\lambda_\alpha(x)=[\lambda_\alpha(x)]^{\dagger} . \tag{2.8}$$

Consequently, we see that

$$(\bar{\lambda}^T)_\alpha=-(\gamma^0\lambda)_\alpha , \tag{2.9}$$

where $\bar{\lambda}=\lambda^T\gamma^0$ and the transpose operation (T) is with respect only to the spinor indices. Equations (2.7) and (2.8) are consistent with the plane-wave representation[3]

$$\lambda(x)=\frac{1}{(2\pi)^3}\int\frac{d^3k}{2\omega_k}\sum_{\pm}[b_\eta(q)u(q,\eta)e^{-iq\cdot x} + b^{\dagger}_\eta(q)v(q,-\eta)e^{iq\cdot x}] , \tag{2.10}$$

where $\omega_k=|\mathbf{k}|$ and here the plane-wave spinors refer to zero mass.

III. PROPAGATORS AND VERTICES

In this section we sketch the development of what can be regarded as the conventional form[3,4] of the Feynman rules associated with $\mathcal{L}_{WZ}$ in order to indicate some of the difficulties that accompany their use. The graphical rules for the pure QED and quadratic parts of $\mathcal{L}_{WZ}$ are standard[8] so that we need confine our attention to only the Majorana pieces of $\mathcal{L}_{SY}$ and $\mathcal{L}_G$.

We consider first the $\psi\psi\rightarrow SS$ (or PP) tree graph depicted in Fig. 1. When Wick's theorem is straightforwardly applied to the relevant four-point function one encounters a fermion-number-nonconserving $\bar{\lambda}\bar{\lambda}$-type propagator[9]

$$\langle 0\,|\,T[\bar{\lambda}(x)_\alpha\bar{\lambda}(y)_\beta]\,|\,0\rangle=-i[\gamma^0 S_F(x-y)]_{\alpha\beta} , \tag{3.1}$$

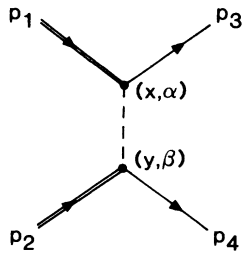

FIG. 1. Tree graph for $\psi\psi\rightarrow SS$ (or PP). The double (dashed) lines refer to Dirac (Majorana) fermions. The solid lines refer to either scalar (S) or pseudoscalar (P) particles. The external momenta are p_i. The vertices are labeled by a space-time point and a spinor index, respectively.

that is represented graphically in Fig. 2(c). The vertices appropriate to this propagator assignment follow immediately from (2.4) and the standard algorithms[10] yielding [Fig. 3(a)]

$$-iQ\bar{\lambda}(1,i\gamma_5)\psi(S^{\dagger},P^{\dagger})\sim+Q(1,i\gamma_5)\delta_{\alpha\beta} . \tag{3.2}$$

Similarly, we see that

$$iQ\bar{\psi}(1,i\gamma_5)\lambda(S,P)\sim-Q(1,i\gamma_5)\delta_{\alpha\beta} , \tag{3.3}$$

corresponding to the vertex in Fig. 3(b). It is important to keep in mind that there is a certain degree of arbitrariness in the propagator and vertex assignments that results from the self-conjugacy of Majorana fermions. The choices depicted in Figs. 2 and 3 are associated with a possibility that we refer to as nonfermion-flow perturbation theory.

If the initial Dirac operators are taken[11] in (1,2) order

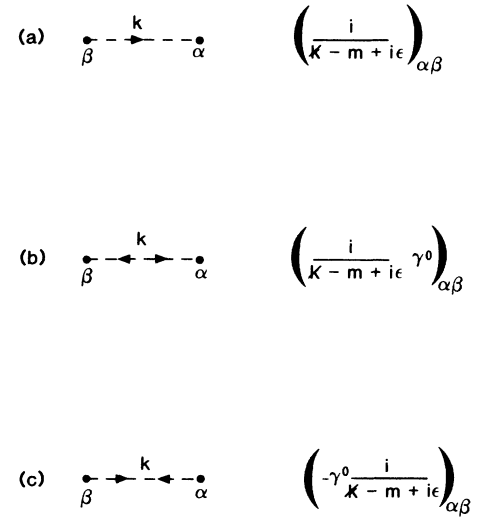

FIG. 2. Propagators for a Majorana fermion of mass m in nonfermion-flow perturbation theory. The direction of momentum flow (k) is from left to right as labeled by the four-component spinor indices β and α, respectively.

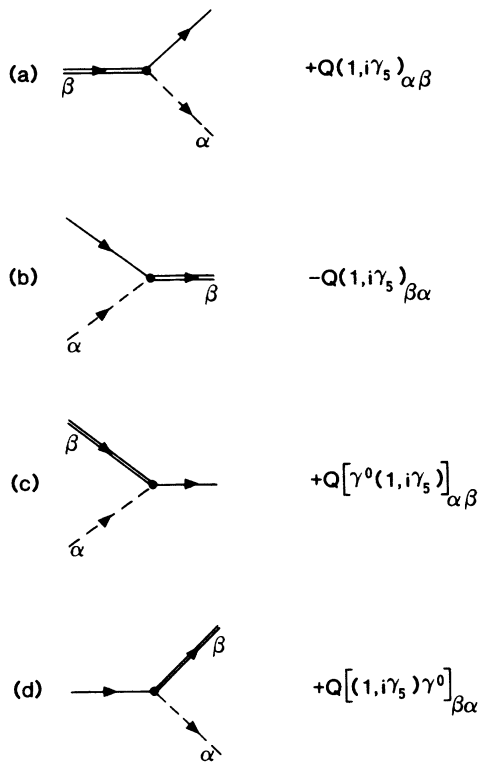

FIG. 3. Majorana-Dirac-scalar vertices in nonfermion-flow perturbation theory.

in the underlying time-ordered (τ) product and the conventional ($\psi\bar{\psi}$) ordering for the contraction is associated with the Dirac propagator, then (3.1) represents the order of the Majorana contraction when the overall permutation signature is even.[12] The momentum flow through the internal Majorana line in this instance is from vertex y to vertex x. Thus we obtain the amplitude

$$M(\text{Fig. } 1) = -iQ^2\bar{v}(p_1)\frac{1}{\not k}u(p_2)\ , \tag{3.4}$$

where $k=p_2-p_4$. In this calculation as well as in all others throughout this paper we adhere to the standard assignments[7] of spinor wave functions to external fermion lines. Thus, Eq. (3.4) is our first indication that perhaps there is another way to think about the fermion flow patterns in Fig. 1.

The vertex assignment depicted in Fig. 3(c) can be determined by insisting that one obtain (3.4) using any one of the three Majorana propagators shown in Fig. 2 provided the momentum flow is the same in each case. Alternatively, since the vertex in Fig. 3(c) is a λ-reversed version of the one in Fig. 3(a) and because

$$-iQ\bar{\lambda}(1,i\gamma_5)\psi(S^\dagger,P^\dagger) = -iQ\lambda^T\gamma^0(1,i\gamma_5)\psi(S^\dagger,P^\dagger)\ , \tag{3.5}$$

we can immediately infer the appropriate vertex assignment.

The overall sign of (3.4) changes if we reverse the direction of the momentum flow k (Ref. 13). Because Majorana fermions carry no superselective quantum number such as lepton number there is no natural association of their fermionic and momentum flows. As a consequence, the graphical rules depicted in Figs. 2 and 3 leave the overall sign of a graph containing Majorana fermions indeterminate over and above the usual[12] signature ambiguity of any graph containing fermions. Generally this sign must be known relative to other coherent amplitudes either of equal or higher order in the coupling. The statements of the graphical rules in Refs. 3 and 4 offer what appear to be uncertain counsel in circumstances such as these. The principal problem is that, in general, the direction of the momentum flow through Majorana lines differs among graphs contributing coherently to an amplitude.

The remaining vertex [Fig. 3(d)] of the two λ-reversed vertices can be determined by considering the lowest-order Majorana-exchange contribution to $\psi S(P) \rightarrow \psi S(P)$ shown in Fig. 4(a) and again imposing invariance with respect to the choice of Majorana propagator. Alternatively, Fig. 3(d) is the λ-reversed form of Fig. 3(b) so

$$iQ\bar{\psi}(1,i\gamma_5)\lambda(S,P) = -iQ\bar{\psi}\gamma^0(1,i\gamma_5)\bar{\lambda}^T(S,P)\ , \tag{3.6}$$

from which one infers the correct vertex assignment.

The complete tree-graph contribution to $\psi S(P) \rightarrow \psi S(P)$ provides a good example of the necessity of a proper choice of the direction of momentum flow. In this case the correct choice is in the direction $k=p_4-p_2$, if we adhere to the sign convention implicit in the use of the standard Feynman rules for the photon-exchange contribution Fig. 4(b). This last convention is set by the ordering that is presupposed for the initial and final Dirac particles in the associated four-point function; we note that the sign of the amplitude

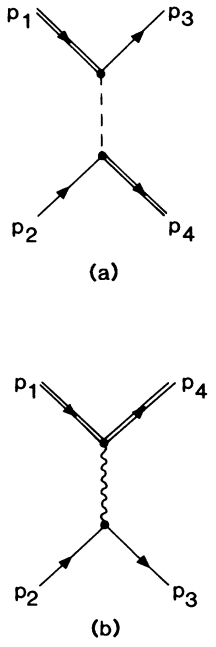

FIG. 4. Tree graphs for $\psi S(P) \rightarrow \psi S(P)$. The wavy line represents a photon.

representing Fig. 4(b) is independent of the sign of the exchanged momentum. We will have more to say about implicit sign conventions in the next section.

This set of nonfermion-flow Majorana Feynman rules[3,4] is completed by assigning a factor of $\frac{1}{2}$ to each closed Majorana loop because of exchange symmetry and by extending the class of vertices to models that have vector-Dirac-Majorana as well as boson-Majorana-Majorana couplings. We consider these extensions in the Appendix. We note that some ordering ambiguities associated with two-Majorana vertices have been discussed in detail by Haber and Kane.[4] Our rendition of this class of vertices is quite different.

IV. SIGNATURE AMBIGUITIES

In the preceding section we encountered a familiar signature ambiguity in dealing with the graphs of Fig. 4 that is easily resolved by adapting a standard ordering convention for the fermions and the usual association of the direction of momentum and fermion flow with contraction order. A different kind of signature problem appears in Majorana fermion graphs such as Fig. 1 through which it is not possible to trace a continuous line of fermion flow without reversing the customary associations for Dirac lines. The tree graphs for the process $SS \to \psi S \lambda$ shown in Fig. 5 provide richer examples of the consequences of this distinctive feature of graphs containing Majorana fermions. In the calculations associated with these and all other graphs containing external Majorana lines we always have the option of regarding the Majorana fermion either as outgoing with momentum p_s (say) or incoming with momentum $-p_s$.

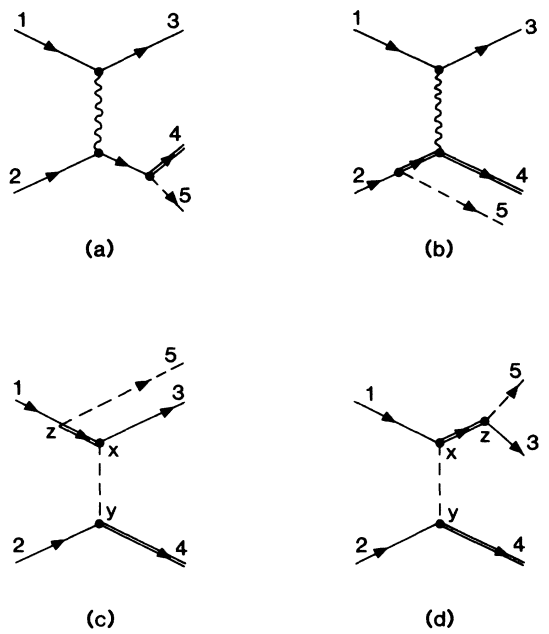

FIG. 5. Tree graphs for the process $SS \to \psi S \lambda$. The complete tree-graph amplitude is obtained by considering the $(1 \leftrightarrow 2)$-crossed graphs as well.

The assignment of the external spinor wave function follows our general rule,[7] for example, corresponding to the outgoing [incoming] final-state external Majorana line we have $\bar{u}(p_s)$ $[v(p_s)]$. The vertex assignments are, of course, different for each of the Majorana fermion directionalities.

The overall signs of the amplitudes corresponding to even the relatively simple graphs shown in Figs. 5(a) and 5(b) obviously depend upon the ordering of the $\lambda(5)$ and $\psi(4)$ operators in the appropriate time-ordered product. On the other hand, the standard QED rules along with the vertex assignment of Fig. 3(d) imply definite overall signs for these contributions to the amplitude. The reason for this is that a signature convention is always implicit when the customary vertex assignments are utilized. This convention takes as a criterion for the positivity of the parity of any permutation a certain standard ordering of the fermion operators. This is the order obtained after all of the fermion operators have been contracted into what may be taken to be naturally ordered pairs. In such a pair the right-to-left ordering of the operators corresponds to an order of points on the graph in the direction of momentum flow.[14] It is with such a convention that the propagators on the external lines are pulled off the tree-level three-point function in order to extract the point vertex. We refer to this as the *even-parity convention* (EPC).

In connection with Fig. 5(a) the EPC corresponds to the ordering $\lambda(5)\psi(4)$ in the τ product which must be retained for the remaining graphs in order to ensure the correct relative signs among the different amplitudes. This is obvious for Fig. 5(b), but less so for Figs. 5(c) and 5(d) where one must deal with the problem of the direction of flow through the Majorana internal lines.

It is evident from Fig. 5(c) that contractions with the fermion operators appearing in the interactions represented by the points x and y are consistent with the EPC if the fermion flow coincides with the momentum flow from the point z through the external line 4 so that standard fermion propagators can be assigned to the directed lines $z \to x$ and $x \to y$. With the EPC the momentum associated with the internal Majorana line in Fig. 5(c) therefore must be $p_4 - p_2$ and must flow in the direction $x \to y$. This is, by the EPC, consistent with a definite direction of momentum flow through the Majorana internal line in Fig. 5(d) but this direction is not graphically obvious. One finds that the correct momentum in this case is $p_2 - p_4$, namely, the reverse of what is in Fig. 5(c).

Our final example involving the tree-level graphs for $\psi\psi \to \psi S \lambda$ that are shown in Fig. 6 contains a more familiar signature question resulting from the crossover of fermion lines. Here the EPC is consistent with a (5,3)(1,2) ordering of the fermion operators. The calculation of the amplitudes represented by the graphs of Figs. 6(a) and 6(b) is routine. This is because the fermion lines trace a continuous fermion flow, as indicated in Figs. 7(a) and 7(b), and also because the direction of momentum flow through the photon line is immaterial to the sign of the amplitude. We refer to diagrams such as shown in Fig. 7 as fermion skeleton graphs.

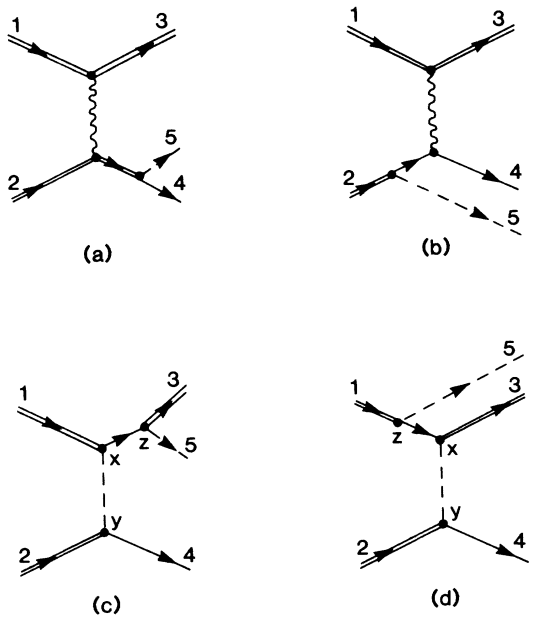

FIG. 6. Tree graphs for the process $\psi\psi\rightarrow\psi S\lambda$. The complete tree-graph amplitude is obtained by considering the $(1\leftrightarrow 2)$-crossed graphs as well with an overall negative relative phase.

In Fig. 6(c) we encounter the archetypical graph involving Majorana fermions where there are lines of discontinuous fermion flow, at least in the usual sense. The ordering of contractions implicit in the EPC can be represented as in Fig. 7(c). A depiction with the flows $1\rightarrow 2$ and $3\rightarrow 5$ would be equally representative, as would the flows $2\rightarrow 1$ and $3\rightarrow 5$, provided we associate no rules for determining amplitudes from these graphs. Our objective in the next section is to formulate such rules; it is with this in mind we have taken the EPC to correspond to fermion flows with the same senses of initial and final states on each of the lines as in Figs. 7(a) and 7(b), whether or not they cross. We do indeed encounter crossing in representing the fermion flows in Fig. 6(d) in a similar manner [Fig. 7(d)]. This means, as in any fermion-containing amplitude, when a change of the standard ordering takes place we pick up an overall sign onto the amplitude one obtains by applying the standard graphical algorithm to Fig. 6(d) assuming the EPC which obviously implies a momentum flow p_2-p_4 through the internal Majorana line. For n crossings of the fermion flow lines one evidently picks up an overall factor of $(-1)^n$ onto an amplitude that is calculated using an EPC-implicit set of rules.

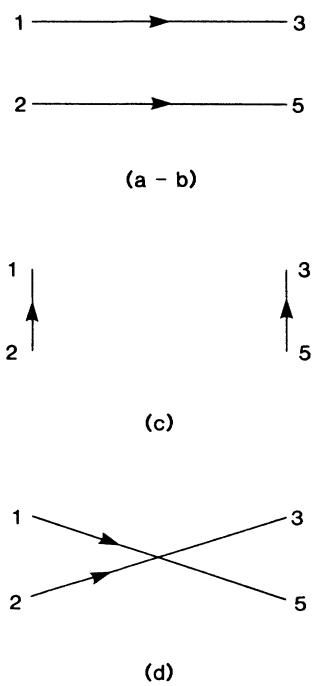

FIG. 7. Fermion-flow skeleton graphs corresponding to the tree graphs in Fig. 6.

In this section and in the preceding one we have illustrated by several examples the signature uncertainties that are peculiar to graphs containing Majorana fermions when the usual set[3,4] of Feynman rules is used. In the next section we develop a new set of rules wherein sign problems are reduced to the familiar type that are encountered in dealing with any graph containing fermions.

V. NEW MAJORANA FEYNMAN RULES

The root of the various unusual aspects of the preceding Majorana Feynman rules is, of course, Majorana fermion self-conjugacy. For more elaborate models this can result in a picturesque assortment of propagators and vertices at least an order of magnitude more numerous than if there were only Dirac fermions carrying superselective quantum numbers. A new and inconvenient problem attendant to these Majorana rules is that of distinctive relative signature ambiguities among coherent amplitudes that apparently cannot be resolved graphically within the context of the rules. In this section we show that with an alternative and simpler set of Majorana Feynman rules, the relative sign problem reduces to the usual one encountered with fermions.

The plurality of Majorana propagators (Fig. 2) is accommodated in the nonfermion-flow version of the Majorana Feynman rules by introducing the λ-reversed vertices appearing in Figs. 3(c) and 3(d). There is an alternative to this which is to insist that Majorana internal lines correspond only to the conventional fermion propagator depicted in Fig. 2(a) along with the stipulation that all articulated fermion segments represent a continuous line of fermion flow. One then encounters formal[15] vertices where *both* the Majorana fermion and the Dirac fermion are reversed such as the one implicit in the fermion flow skeleton graph of Fig. 7(c) that is abstracted from Fig. 6(c). The important question is whether this is a useful thing to do.

In place of Eq. (3.5) we note that

$$-iQ\bar{\lambda}(1,i\gamma_5)\psi(S^\dagger,P^\dagger)=+iQ\lambda^T(1,i\gamma_5^T)(\bar{\psi}^c)^T(S^\dagger,P^\dagger), \tag{5.1}$$

where $\psi^c \equiv C\bar{\psi}^T$ so that with our choice of C and in the Majorana representation we have

$$\psi^c_\alpha = \psi^\dagger_\alpha , \tag{5.2}$$

for each of the spinor indices α. Once we reverse a Dirac fermion line within a graph, it will either stop at a Dirac-Majorana-vertex or continue its way out on an external line. Its progress at each step of the way is represented by normal Dirac propagators, with a reversed sense, that represent contractions of the ψ^c and $\bar{\psi}^c$ operators. The various factors of γ^0 that occur in the previous propagators and vertices are absorbed in this turning of the Dirac lines along with changes in the external-line assignments from u and $\bar{u}$ to $\bar{v}$ and v, respectively. In this connection we note that (sums over λ and κ)

$$\psi^c_\alpha(x)\bar{\psi}^c_\beta(y) = \gamma^0_{\alpha\kappa}\psi_\lambda(y)\bar{\psi}_\kappa(x)\gamma^0_{\lambda\beta} , \tag{5.3}$$

so the contraction of $\psi^c_\alpha(x)\bar{\psi}^c_\beta(x)$ is $[S_F(x-y)]_{\alpha\beta}$. Also we recall that $\bar{u}_\alpha = -(\gamma^0 v)_\alpha$ and $\bar{v}_\alpha = -(\gamma^0 u)_\alpha$.

A straightforward way to determine the correct vertex assignment corresponding to Fig. 8(c) and the EPC is to calculate the amplitude corresponding to Fig. 3(a) with both fermions on shell and then rewrite the result as indicated in the preceding discussion. This leads to the vertex assignment shown in Fig. 8(c). Interestingly, this result is identical to what one would naively infer from (5.1) if the fermion fields commuted, rather than anticommuted, so that the right-hand side would be

$$+iQ\bar{\psi}^c(1,i\gamma_5)\lambda(S^\dagger,P^\dagger) . \tag{5.4}$$

The standard algorithms[10] can then be applied to (5.4) with respect to the conjugate fields.

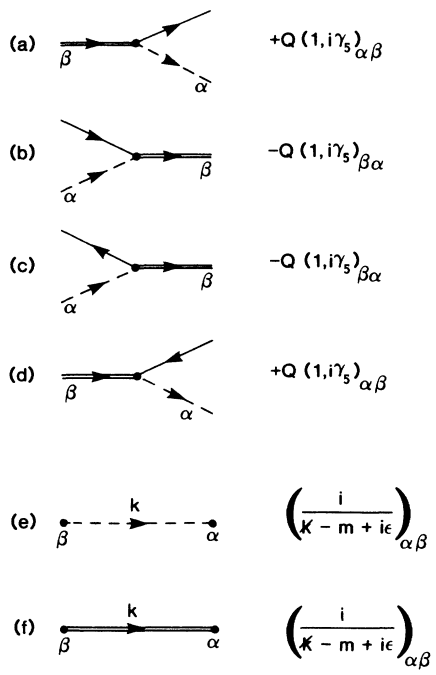

FIG. 8. Vertex and propagator assignments for fermionic-flow Majorana Feynman rules.

Similarly, in place of (3.6) we can write

$$iQ\bar{\psi}(1,i\gamma_5)\lambda(S,P) = -iQ(\psi^c)^T(1,i\gamma_5)\bar{\lambda}^T(S,P) , \tag{5.5}$$

to which we associate the vertex depicted in Fig. 8(d) by the same procedure that led to Fig. 8(c). The "normal" vertices, shown again in Figs. 8(a) and 8(b), represent the left-hand sides of Eqs. (3.2) and (3.3), respectively, just as they did before.

We next reconsider the processes in Fig. 1 and Figs. 4–6 using the fermion-flow graphical rules for Majorana fermions. We notice that the fermion-flow skeleton graph corresponding to Fig. 1 and the EPC with the initial order again taken as (1,2) is simply the line on the left-hand side of Fig. 7(c). Figure 1 is redrawn in Fig. 9 to further illustrate the new rules and the association with Eq. (3.4) is then immediate. In the case of $\psi S(P) \to \psi S(P)$ (Fig. 4) the obvious line of fermion flow from the initial out through the final Dirac legs is consistent with the EPC; we note the congruence of the fermion flows in Figs. 4(a) and 4(b).

Figure 5(a), although devoid of the complications of fermion propagators tests the EPC. As drawn the Majorana-Dirac-scalar vertex in Fig. 5(a) is associated with Fig. 3(d) in the nonfermion-flow rules. In the fermion-flow case, either the vertex of Fig. 8(b) or of Fig. 8(d) seems to apply, and in fact, in all three cases we obtain the factor $Q\bar{u}(p_5)v(p_4)$ as the contribution to the amplitude from this portion of the graph. However, the EPC for this graph corresponds to the ordering (5,4) which is represented graphically by Fig. 8(b). We can deduce the EPC for this process graphically by noting that in situations where an external Dirac fermion and an external Majorana fermion, both in the initial or final state, are connected by an internal fermion line containing no Majorana propagators [such as in Figs. 5(a) and 5(b)] the EPC corresponds to reversal of the external Majorana line. While the direction of flow is irrelevant in determining the correct amplitudes for this process, in many cases it is crucial that the EPC be employed correctly. Thus we state a general convention that for vertices with an external Dirac fermion and an external Majorana fermion both going into the future, we will always choose the vertex shown in Fig. 8(b), and for both coming from the past the vertex in Fig. 8(a) will be used.

The remaining graphs in Fig. 5 will also correspond to the same fermion flow in through the line 5 and out

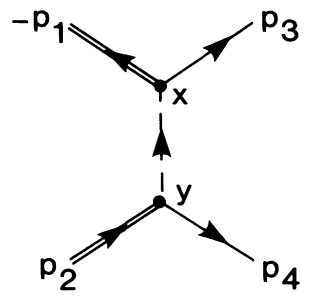

FIG. 9. Fermion-flow counterpart of Fig. 1.

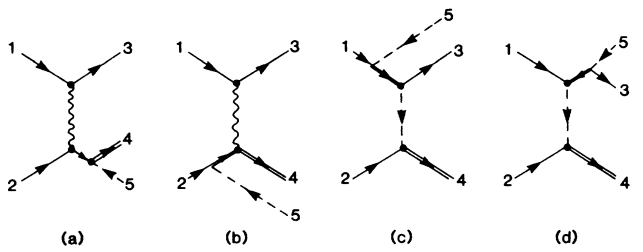

FIG. 10. Fermion-flow counterparts of Figs. 5(a)–5(d).

through the line 4, consistent with the EPC, as shown in Fig. 10. The simplification over our earlier treatment should be evident.

Figure 6 presents an interesting challenge. The crucial aspect is to be consistent with the EPC to within an overall sign on all of the amplitudes in drawing the fermion flows. This can be done in a number of practical ways. Our original ordering of fermion operators was $(5,3,\bar{1},\bar{2})$ where we have used an overbar to distinguish the quantities referring to the initial state. Figures 6(a)–6(d) correspond to the subgroupings (5,2)(3,1), (5,2)(3,1), (5,3)(1,2), and (5,1)(3,2) respectively. Only the last one is an odd permutation from the standard order which accounts for the $(-1)^c$, $c=1$, crossover parity. The general rule we have been developing amounts to the requirement that each graph be grouped into EPC-consistent fermion lines, the revised Majorana rules are then applied, and finally, a crossover parity is supplied to each graph. The EPC-consistent fermion-flow lines are indicated in the redrawn graphs of Fig. 11.

The application of the rules to Fig. 6 is immediately clear except for Fig. 6(c). The EPC-consistent ordering deduced from Figs. 6(a) and 6(b) could equivalently be either (5,3)(1,2) or (3,5)(2,1). The equivalence of these two orderings in the Wick expansion is seen graphically in Figs. 6(a), 6(b), and 6(d), where the flow is unambiguously from initial to final particle states. In Fig. 6(c), however, the flow is between two particles in the same (either initial or final) state. Here the two orderings are not equivalent graphically. As pointed out above, the amplitude of the graph is independent of the direction of fermion flow between 3 and 5. On the other hand, the overall sign of the graph certainly depends upon the direction of fermion flow between 1 and 2. The need for caution in applying the EPC to graphs containing vertices such as the 3-z-5 vertex in Fig. 6(c) is now apparent. Using the general convention stated earlier, we choose a (5,3) ordering for the final-state fermions (fermion flow from 5 to 3), which immediately requires a (1,2) ordering for the initial-state particles. This result, depicted in Fig. 11(c), leads to the correct signature for this contribution to the overall amplitude.

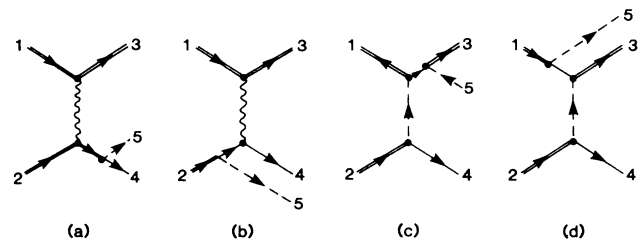

FIG. 11. Fermion-flow counterparts of Figs. 6(a)–6(d).

VI. CONCLUSIONS

We have established that there is a simpler alternative to the Feynman rules for Majorana fermions previously proposed in the literature.[3,4] The present rules more closely resemble those for Dirac fermions in that they involve only a single type of propagator and a reduced number of vertices that are free of any appended charge conjugation matrices and, moreover, have well-defined graphical fermion flows. Other proposals for Majorana Feynman rules allow nonfermion-flow graphical structures.

Some of the new vertices [cf. Figs. 8(c) and 8(d)] seem to violate charge conservation as a consequence of our reversal of some Dirac lines into their charge conjugates, but this presents no difficulties in practice. The vertex and wave-function assignments along with the reversal of momentum flow through the propagator always compensate for what may appear to an incorrect flow of charge. In a sense, we have traded the usual depiction of charge flow for the preservation of the articulated fermion flow typical of graphical rules involving only Dirac fermions.

The loss of the usual charge-flow feature is inconsequential. On the other hand, there seems to be a definite gain from insisting on the fermion-flow characteristic in resolving some of the unusual relative signature ambiguities that appear in problems with Majorana fermions. A few of these signature problems seem to have been unnoticed previously. They are related to the lack of a conserved quantum number carried by the Majorana fermions and to the linearity in momentum of the inverse of any fermion propagator. Therefore, these ambiguities are not resolved by regarding the Majorana fields as four-dimensional versions of Weyl fields.

The new rules involve only the relative signature problems one expects in any process involving fermions. A key tool in our analysis of these signature problems is what we have referred to as the *even-parity convention* which sets a permutation parity standard for vertex assignments involving any types of fermions, Majorana or not.

This investigation provides some interesting insights into the graphical associations that are made in formulating Feynman rules for fermions. Our principal result, however, is a set of rules for Majorana fermions with which practical calculations appear to be considerably simpler and less ambiguous than other alternatives.

ACKNOWLEDGMENTS

This work was supported in part by the U.S. National Science Foundation and by the U.S. Department of Energy, Division of High Energy Physics, Contract No. W-31-109-ENG-38. One of us (E.I.G.) would like to

thank the High Energy Theory Group at Argonne for its hospitality during a visit in which part of this work was carried out as well as the Division of Educational Programs at Argonne for its support. We also thank C. L. Bilchak, G. Eilam, and E. Reya for helpful comments.

APPENDIX

The Wess-Zumino model does not involve vertices with two Majorana fermions or vertices with a vector boson coupled to a Dirac fermion and a Majorana fermion. A more comprehensive model is provided by the generic Majorana-interaction Lagrangian[4]

$$\mathcal{L}_{\rm MI}=\tfrac{1}{2}g^i_{abc}\bar{\lambda}_a\Gamma_i\lambda_b\phi_c+\tfrac{1}{2}g^{i*}_{abc}\bar{\lambda}_b\Gamma_i\lambda_a\phi^\dagger_c + k^i_{abc}\bar{\lambda}_a\Gamma_i\psi_b\phi^\dagger_c+k^{i*}_{abc}\bar{\psi}_b\Gamma_i\lambda_a\phi_c\ . \tag{A1}$$

We have followed the conventions of Ref. 4 in writing out (A1). The fermionic kinetic energies, $\frac{1}{2}i\bar{\lambda}_a(i\partial\!\!\!/ - M_a)\lambda_a$ and $\bar{\psi}_a(i\partial\!\!\!/ - m_a)\psi_a$, corresponding to the various Majorana (λ_a) and Dirac (ψ_a) fields, respectively, are *added* onto $\mathcal{L}_{\rm MI}$ in addition to the bosonic and boson-Dirac-interaction pieces to form the complete Lagrangian. The indices a,b,c, which are summed when repeated, refer to distinct particle types and, for the vector field, a Lorentz index as well, that is implicitly contracted with the index i which arises in connection with the linearly independent combinations of gamma matrices and their products represented by the Γ_i, $i=1,\ldots,16$. Generally, $C^{-1}\Gamma_iC=\eta_i\Gamma_i^T$, where $\eta_i=+1$ for $\Gamma_i=1,i\gamma_5,\gamma_\mu\gamma_5$ and $\eta_i=-1$ for $\Gamma_i=\gamma_\mu,\sigma_{\mu\nu}$. The g^i_{abc} are constrained by fermion anticommutivity to be either symmetric or antisymmetric in a and b.

A full set of Majorana nonfermion-flow Feynman rules predicated on the use of the three different Majorana propagators shown in Fig. 2 and $\mathcal{L}_{\rm MI}$ is given in Ref. 4.

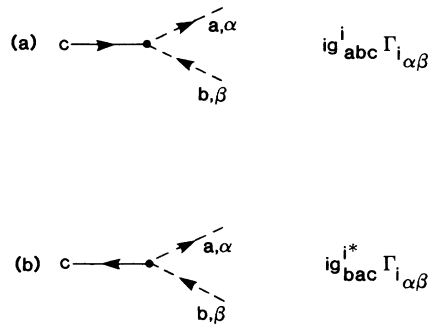

FIG. 12. Fermion-flow Majorana-Majorana-boson vertices.

There appear six different ϕ-λ-λ vertices. The four different kinds of ϕ-λ-ψ vertices are identical to those depicted in Fig. 3, although the vertex assignments of course correspond to more general gamma-matrix structures.

The fermion-flow Majorana Feynman rules entail only the two vertices of Fig. 12. Again it is important to keep in mind the EPC implicit in all vertex assignments involving fermions. This sort of ambiguity was noticed by Haber and Kane for $\bar{\lambda}$-λ-ϕ-type vertices who then analyzed a nonfermion-flow vertex with two outgoing Majorana fermions for which the problem is particularly striking.

Finally, let us deal with the generalizations of the vertices appearing in Fig. 8 corresponding to the Majorana-Dirac-boson terms in (1.1) and the associated ψ-reversed forms. The depiction of the vertices is exactly as in Figs. 8(a)–8(d), but now with the more general vertex assignments, $ik^i_{abc}(\Gamma_i)_{\alpha\beta}$, $i(k^i_{abc})^*(\Gamma_i)_{\beta\alpha}$, $-ik^i_{abc}\eta_i(\Gamma_i)_{\beta\alpha}$, and $-i(k^i_{abc})^*\eta_i(\Gamma)_{\alpha\beta}$, respectively.

---

*On leave from the Department of Physics, Case Western Reserve University, Cleveland, OH 44106.

[1]B. Kayser, Phys. Rev. D **30**, 1023 (1984), and references cited therein. For descriptions of the experimental situation see F. T. Avignone *et al.*, *ibid.* **35**, 1713 (1987); (unpublished); D. O. Caldwell *et al.* (unpublished).

[2]We are aware of only two discussions (Refs. 3 and 4) of the special properties of Majorana Feynman rules that compare in clarity and completeness to textbook listings of the rules for theories containing Dirac fermions.

[3]S. K. Jones and C. H. Llewellyn-Smith, Nucl. Phys. **B217**, 145 (1983).

[4]H. E. Haber and G. I. Kane, Phys. Rep. **117**, 76 (1985).

[5]R. W. Brown and K. L. Kowalski, Phys. Lett. **144B**, 235 (1984).

[6]J. Wess and B. Zumino, Nucl. Phys. **B70**, 39 (1974); Phys. Lett. **49B**, 5 (1974); Nucl. Phys. **B78**, 1 (1984).

[7]C. Itzykson and J.-B. Zuber, *Quantum Field Theory* (McGraw-Hill, New York, 1980), Appendix A.

[8]See, for example, Ref. 7. The conventions employed in Ref. 5 are the same in this respect and also involve the use of the Feynman gauge in the QED sector.

[9]We note that $(\bar{\lambda})_\alpha=(\bar{\lambda}^T)_\alpha=(\gamma^{0T}\lambda)_\alpha$; e.g., cf. Ref. 3.

[10]T.-P. Cheng and L.-F. Li, *Gauge Theory of Elementary Particle Physics* (Oxford University Press, New York, 1984), Appendix B.

[11]We follow Fig. 1 in labeling the external lines. Thus (1,2) refers to the operator product $\bar{\psi}(1)\bar{\psi}(2)$ appearing in the relevant τ function.

[12]See Ref. 7, p. 273 and Ref. 10 for discussions of the determination of the overall signs of amplitudes which involve fermions.

[13]This is true whether or not the Majorana fermion has mass.

[14]For example, if we use square brackets to indicate the contraction operation, then $[\psi(x)\bar{\psi}(y)]$ corresponds to momentum flow from y to z.

[15]The purely formal aspect of the associations with the interaction vertices is readily apparent from the fact that the directionalities of the Dirac legs of these new vertices do not coincide with the directionality of the flow of charge.